

Mechanistic Information on the Redox Cycling of Nickel(II/III) Complexes in the Presence of Sulfur Oxides and Oxygen. Correlation with DNA Damage Experiments

Vasilios Lepentsiotis,[†] Joanna Domagala,^{†,‡} Irena Grgic,^{†,§} Rudi van Eldik,^{*,†} James G. Muller,^{||} and Cynthia J. Burrows^{*,||}

Institute for Inorganic Chemistry, University of Erlangen-Nürnberg, Egerlandstrasse 1, 91058 Erlangen, Germany, and Department of Chemistry, 315 S. 1400 East, University of Utah, Salt Lake City, Utah 84112-0850

Received November 20, 1998

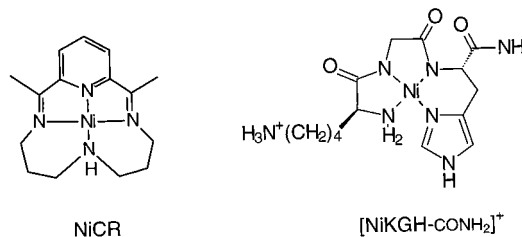
The reactions of the water-soluble complexes $[\text{NiCR}]^{2+}$ (where CR = 2,12-dimethyl-3,7,11,17-tetraazabicyclo[11.3.1]heptadeca-1(17),2,11,13,15-pentaene) and $[\text{NiKGH-CONH}_2]^+$ (where KGH-CONH₂ = lysylglycylhistidinecarboxamide) with sulfite/O₂ and peroxymonosulfate have been investigated using spectrophotometric and rapid-scan techniques. In most cases, the spectral changes suggest the formation of an intermediate Ni(III) species, followed by decomposition reactions which involve a back-reaction to Ni(II). Only in the case of the $[\text{NiCR}]^{2+}$ –S(IV)–O₂ system is the formed Ni(III) species stable in solution. When sulfite and oxygen are used to oxidize Ni(II) to Ni(III), the reaction is oxygen dependent and an induction period could be observed, whereas the use of the strong oxidizing agent peroxymonosulfate resulted in no induction period and no oxygen dependence. In addition, the oxidation of Ni(II) to Ni(III) was faster if peroxymonosulfate was used instead of sulfite/O₂. The $[\text{NiKGH-CONH}_2]^+$ complex reacts much faster with sulfite/O₂ and peroxymonosulfate than the $[\text{NiCR}]^{2+}$ does. Rate constants for the oxidation process and possible reaction mechanisms, based on available literature data, that can account for the observed kinetic observations in a qualitative way are presented, and the results are correlated with previously obtained data on DNA modification using these systems.

Introduction

The metal-catalyzed autoxidation of sulfur(IV) oxides plays an important role in environmental atmospheric chemistry (acid rain formation), as well as in biochemistry. Human exposure to sulfite arises either from inhalation of SO₂, largely from industrial emissions,^{1–3} or from ingestion of the aquated form, SO₃²⁻/HSO₃⁻, that is present as a preservative in food, alcoholic beverages, or drugs.^{2,4} A number of toxic effects are associated with sulfite including asthma, mutagenesis or comutagenesis, and the ability to act as a cocarcinogen.^{2,5} Sulfite can also undergo autoxidation to the very reactive peroxymonosulfate (HSO₅⁻).³

Although the mechanistic details of sulfite toxicity are not completely understood, several studies have suggested sulfur oxy radicals (SO₃^{•-}, SO₄^{•-}, or SO₅^{•-}) as potential oxidants of cellular components including cell membranes, proteins, and DNA.^{1–3} The generation of these radicals from oxidation of sulfite can be catalyzed by enzymes⁶ or transition metal complexes^{3,7–12} or can be uncatalyzed.^{3,13} Recently, it was

observed that $[\text{NiCR}]^{2+}$ (CR = 2,12-dimethyl-3,7,11,17-tetraazabicyclo[11.3.1]heptadeca-1(17),2,11,13,15-pentaene) in the presence of KHSO₅ induced a guanine-specific oxidation of DNA with SO₄^{•-} being the reactive species.¹⁴ In a further study the use of the $[\text{NiKGH-CONH}_2]^+$ complex (where KGH-CONH₂ = lysylglycylhistidinecarboxamide) in the presence of ambient O₂ and 100 μM Na₂SO₃ resulted also in a guanine-specific modification of DNA.¹⁵ This study represented the first observation of DNA damage by a Ni(II) complex in the presence of sulfite and oxygen. Experiments with radical scavengers demonstrated that HSO₅⁻ and SO₄^{•-} are implicated as important intermediates in this process,¹⁵ and an overall reaction mechanism based on earlier results^{3,7} was proposed.



In the present study we have investigated the kinetics and mechanism of the reactions between the two Ni(II) complexes mentioned above and HSO₃⁻/SO₃²⁻ or HSO₅⁻ in the presence

[†] University of Erlangen-Nürnberg.

[‡] On leave from the Institute of Chemistry, University of Wrocław, Poland.

[§] On leave from the National Institute of Chemistry, Ljubljana, Slovenia.

^{||} University of Utah.

- (1) Neta, P.; Huie, R. E. *Environ. Health Perspect.* **1985**, *64*, 209.
- (2) Shapiro, R. *Mutat. Res.* **1977**, *39*, 149.
- (3) Brandt, C.; van Eldik, R. *Chem. Rev.* **1995**, *95*, 119 and literature cited therein.
- (4) Hyatsu, H. *Prog. Nucleic Acid Res. Mol. Biol.* **1976**, *16*, 75.
- (5) Reed, G. A.; Curtis, J. F.; Mottley, C.; Eling, T. E.; Mason, R. P. *Proc. Natl. Acad. Sci. U.S.A.* **1986**, *83*, 7499.
- (6) Mottley, C.; Mason, R. P. *Arch. Biochem. Biophys.* **1988**, *267*, 681.
- (7) Coichev, N.; van Eldik, R. *Inorg. Chem.* **1991**, *30*, 2375.

- (8) (a) Fronaeus, S.; Berglund, J.; Elding, L. I. *Inorg. Chem.* **1998**, *37*, 4939. (b) Berglund, J.; Fronaeus, S.; Elding, L. I. *Inorg. Chem.* **1993**, *32*, 4527.
- (9) Bhattacharya, S.; Ali, M.; Gangopadhyay, S.; Banerjee, P. *J. Chem. Soc., Dalton Trans.* **1994**, 3733.

of oxygen. The aim was to gain mechanistic insight into these systems in order to contribute toward a better understanding of the observed DNA damage in the presence of these reagents.

These complexes were selected for detailed study for two reasons. First, both $[\text{NiCR}]^{2+}$ and $[\text{NiKGH-CONH}_2]^+$ have demonstrated interesting applications to DNA oxidation. The $[\text{NiCR}]^{2+}$ complex is a convenient probe of DNA and RNA structure^{16–21} because of its ability to mediate selective oxidation of guanine residues in the presence of either $\text{SO}_3^{2-}/\text{O}_2$ or HSO_5^- . The nickel peptide complex, $[\text{NiKGH-CONH}_2]^+$, carries out similar guanine chemistry and additionally mimics an important metal binding site in proteins containing the N-terminal copper and nickel binding motif, XXH.²² The chemistry of this peptide complex with sulfite is of interest as a model of nickel and sulfite cototoxicity.¹⁵ Second, these two complexes, by virtue of their different redox potentials,¹⁵ were expected to behave differently with respect to their mechanisms of sulfite autoxidation. Here, we report direct spectroscopic evidence for the redox cycling of the Ni(II/III) complexes, which represents an essential aspect of the catalytic function of these species.

Experimental Section

Chemicals of analytical reagent grade (Merck, Fluka, and Aldrich) and deionized ultrapure water were used to prepare all solutions. A phosphate buffer ($\text{Na}_2\text{HPO}_4/\text{KH}_2\text{PO}_4$) was used to adjust the pH at 6.5, and NaCl, to adjust the ionic strength. Samples of $[\text{NiCR}]^{2+}$ and $[\text{NiKGH-CONH}_2]^+$ were prepared as reported in the literature.^{14,15}

UV–visible spectra were recorded on a HP 8452A diode array spectrophotometer or on a Shimadzu UV-2102/3102PC spectrophotometer. Rapid scan measurements were performed on a Bio Sequential SX-17MV stopped-flow reaction analyzer from applied photophysics equipped with a J & M detector connected to a TIDAS 16-416 spectrophotometer. Stopped-flow measurements were performed on a Bio Sequential SX-18MV stopped-flow spectrophotometer. In general, all kinetic traces were recorded at least 5–8 times, and the reported rate constants are the average values calculated for the series of measurements (error limit between 5 and 10%).

Results and Discussion

The redox behavior of the Ni(II) complexes in the presence of $\text{HSO}_3^-/\text{SO}_3^{2-}/\text{O}_2$ and HSO_5^- was studied spectrophotometrically using rapid-scan and stopped-flow techniques where required. Earlier work on these systems revealed spectral evidence for the formation of an intermediate Ni(III) complex, which exhibited a characteristic absorbance band at 367 nm.¹⁵ The formation and decay of such intermediate species as a function of the selected experimental conditions were studied in a time-resolved manner in the present study. The observations enable us to draw some important mechanistic conclusions. We first present the general results obtained for the different reaction

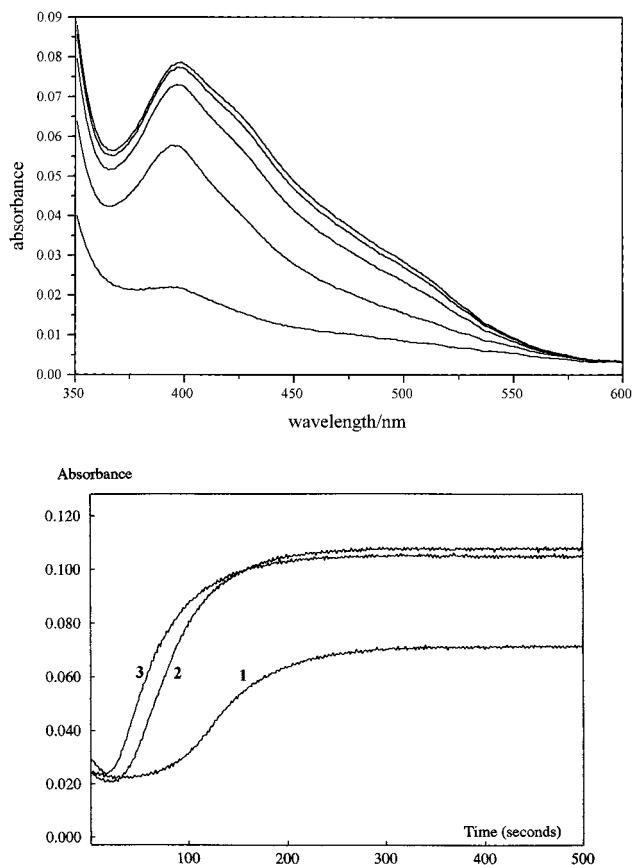


Figure 1. (a) Top: Spectral changes recorded for the reaction of $[\text{NiCR}]^{2+}$ with sulfite in oxygen-saturated solutions. $[\text{NiCR}]^{2+} = 1.25 \times 10^{-4} \text{ M}$; $[\text{S(IV)}] = 1 \times 10^{-3} \text{ M}$; $I = 0.2 \text{ M}$; $\text{pH} = 6.5$; $T = 25 \text{ }^\circ\text{C}$; $\Delta t = 1 \text{ min}$. (b) Bottom: Absorbance–time traces for the reaction of $[\text{NiCR}]^{2+}$ with sulfite in oxygen-saturated solutions at different sulfite concentrations. Key: (1) $[\text{S(IV)}] = 1 \times 10^{-3} \text{ M}$; (2) $[\text{S(IV)}] = 2 \times 10^{-3} \text{ M}$; (3) $[\text{S(IV)}] = 4 \times 10^{-3} \text{ M}$; $\lambda = 390 \text{ nm}$.

systems and then go into a more detailed discussion of the suggested reaction mechanism.

$[\text{NiCR}]^{2+}/\text{HSO}_3^-/\text{SO}_3^{2-}/\text{O}_2$ System. The reaction between $[\text{NiCR}]^{2+}$ and excess sulfite was first studied in the presence of air- and oxygen-saturated solutions at $\text{pH} = 6.5$ ($\text{Na}_2\text{HPO}_4/\text{KH}_2\text{PO}_4$ buffer) using a tandem cuvette. The S(IV) concentration was varied, whereas the $[\text{NiCR}]^{2+}$ concentration ($1.25 \times 10^{-4} \text{ M}$) and the ionic strength (0.2 M with NaCl) were kept constant. In an air-saturated solution and in the presence of 1 mM S(IV), a very slow increase in absorbance around 390 nm was observed. The absorbance vs time trace clearly showed an induction period, and the maximum absorbance was reached after ca. 6 h, which remained constant over a period of 25 h at room temperature. These spectral changes were interpreted as evidence for the slow formation of a stable Ni(III) complex under these conditions.

In oxygen-saturated solutions the reaction is much faster and over within 200 s. Figure 1a shows that the formation of the Ni(III) band at 390 nm, with small shoulders being formed at 430 and 500 nm, is complete within minutes. Stopped-flow measurements were performed at various S(IV) concentrations, for which some typical absorbance vs time traces are reported in Figure 1b. The overall absorbance increase and the formation of Ni(III) strongly depend on the selected sulfite concentration and reach a maximum at 2 mM sulfite. The traces show typical autocatalytic behavior with an induction period that decreases from ca. 90 to ca. 20 s on increasing the sulfite concentration from 0.5 to 4 mM. Following the induction period, a stable Ni(III) complex is formed with a pseudo-first-order rate constant

- (10) Shi, X. *J. Inorg. Biochem.* **1994**, *56*, 155.
- (11) Connick, R. E.; Zhang, Y.-X. *Inorg. Chem.* **1996**, *35*, 4613.
- (12) Muller, J. G.; Burrows, C. J. *Inorg. Chim. Acta* **1998**, *275–276*, 314.
- (13) Connick, R. E.; Zhang, Y.-X.; Lee, S.; Adamic, R.; Chieng, P. *Inorg. Chem.* **1996**, *35*, 4613.
- (14) Muller, J. G.; Zheng, P.; Rokita, S. E.; Burrows, C. J. *J. Am. Chem. Soc.* **1996**, *118*, 2320.
- (15) Muller, J. G.; Hickerson, R. P.; Perez, R. J.; Burrows, C. J. *J. Am. Chem. Soc.* **1997**, *119*, 1501.
- (16) Burrows, C. J.; Rokita, S. E. *Acc. Chem. Res.* **1994**, *27*, 295–301.
- (17) Burrows, C. J.; Rokita, S. E. In *Metal Ions in Biological Systems*; Sigel, H., Sigel, A., Eds.; M. Dekker: New York, 1995; Vol. 33, pp 537–560.
- (18) Shih, H.-C.; Tang, N.; Burrows, C. J.; Rokita, S. E. *J. Am. Chem. Soc.* **1998**, *120*, 3284.
- (19) Burrows, C. J.; Muller, J. G. *Chem. Rev.* **1998**, *98*, 1109.
- (20) Zheng, P.; Burrows, C. J.; Rokita, S. E. *Biochemistry* **1998**, *37*, 2207.
- (21) Hickerson, R. P.; Watkins-Sims, C. D.; Burrows, C. J.; Atkins, J. F.; Gesteland, R. F.; Felden, B. *J. Mol. Biol.* **1998**, *279*, 577.
- (22) Harford, C.; Sarkar, B. *Acc. Chem. Res.* **1997**, *30*, 123.

that is independent of the sulfite concentration and has an average value of $(1.9 \pm 0.1) \times 10^{-2} \text{ s}^{-1}$ under these conditions. It should be noted that the kinetic traces reported in Figure 1b strongly depend on the selected experimental conditions, especially the ratio of the sulfite and oxygen concentrations, and that spontaneous slow decomposition reactions interfere with the reproducibility of the kinetic traces. Variation of the $[\text{NiCR}]^{2+}$ concentration in the presence of an excess of sulfite had no significant influence on the observed rate constant. Addition of excess sulfite to the produced Ni(III) complex resulted in an absorbance decrease and a shift in the absorbance maximum from 390 to 430 nm. The latter spectral changes are assigned to the reduction of Ni(III) to Ni(II) accompanied by the oxidation of the CR ligand (see further Discussion).

The induction period clearly shows an initial small absorbance decrease, which could suggest that the reaction may be initiated by the presence of trace concentrations of Ni(III) in solution. The decrease in the induction period with increasing sulfite concentration as reported in Figure 1b suggests that Ni(III) is reduced by sulfite to Ni(II) to initiate the autoxidation reaction (see suggested reaction mechanism). The rate of this process is expected to depend on the sulfite concentration employed. Experiments performed in the absence of oxygen (i.e. Ar-saturated solution) also showed this initial decrease in absorbance, however, without the subsequent formation of the Ni(III) band. Efforts to increase the Ni(III) concentration of the test solution via addition of some of the product solution to fresh starting solutions revealed no significant influence on the observed kinetic trace in the presence of oxygen. The source of the initial Ni(III) present in solution is presently unknown. It could originate from trace impurities of Fe(III) present in the chemicals used to adjust pH and the ionic strength, as has been suggested for the Mn(II)-catalyzed autoxidation of sulfite.⁸ Alternatively, the initial absorbance decrease may also be related to the formation of a complex between $[\text{NiCR}]^{2+}$ and sulfite prior to the oxidation process (see further Discussion).

$[\text{NiCR}]^{2+}/\text{HSO}_5^-/\text{O}_2$ System. $[\text{NiCR}]^{2+}$ reacts significantly faster with HSO_5^- to form the Ni(III) species than with sulfite in the presence of oxygen. The repetitive scan spectra in Figure 2a,b, recorded at a low and high concentration of HSO_5^- , respectively, along with the absorbance vs time traces in Figure 2c, show that the formation of the Ni(III) band at 400 nm (and shoulder at 500 nm) is complete within a few seconds at high HSO_5^- concentration. No clear induction period was observed, and the fast oxidation process is followed by a slow decomposition reaction, which apparently involves a back-reaction to the Ni(II) complex. The latter reaction is very slow and proceeds only partly at low HSO_5^- concentration, whereas almost a complete redox cycling of the Ni(III) complex is observed at high HSO_5^- concentrations. The final spectrum only shows a broad band/shoulder around 430 nm. This red shift in the product spectrum may be consistent with the overall process involving, ultimately, ligand oxidation to form the CR-2H ligand Ni(II) complex in which a third imine bond has been formed between C10 and N11.²³

To obtain kinetic information on the rate of oxidation and the subsequent reactions, absorbance vs time traces were recorded on different time scales and fitted with different reaction models. On a short time scale, the oxidation reaction that is characterized by an increase in absorbance could be fitted to a single-exponential function. The k_{obs} values, calculated from the absorbance increase only, showed a linear dependence on the HSO_5^- concentration (Figure 3a) with a slope of 87 ± 10

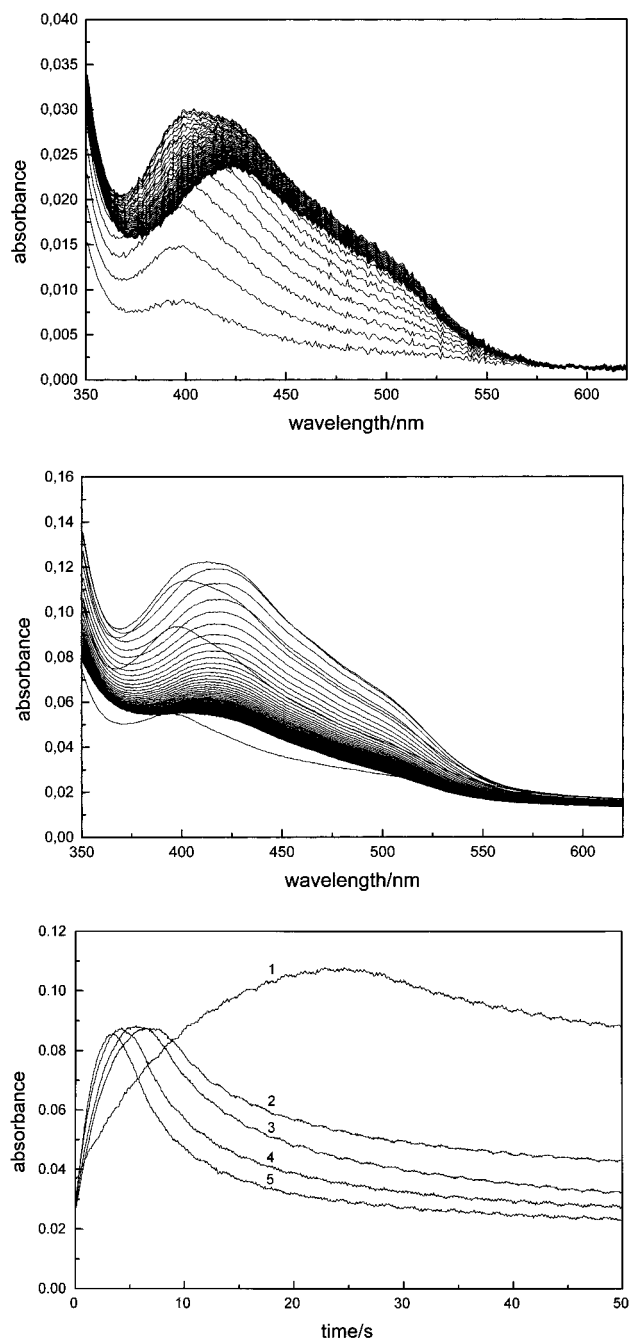


Figure 2. (a) Top: Rapid-scan spectra recorded for the reaction of $[\text{NiCR}]^{2+}$ with peroxymonosulfate in oxygen-saturated solutions. $[[\text{NiCR}]^{2+}] = 1.25 \times 10^{-4} \text{ M}$; $[\text{HSO}_5^-] = 1 \times 10^{-3} \text{ M}$; $I = 0.2 \text{ M}$; $\text{pH} = 6.5$; $T = 25 \text{ }^\circ\text{C}$; $\Delta t = 2 \text{ s}$; optical path length 0.2 cm . (b) Middle: Same except $[\text{HSO}_5^-] = 5 \times 10^{-3} \text{ M}$, $\Delta t \sim 1 \text{ s}$. (c) Bottom: Absorbance–time traces for the reaction of $[\text{NiCR}]^{2+}$ with peroxymonosulfate in oxygen-saturated solutions at different HSO_5^- concentrations. Key: (1) $[\text{HSO}_5^-] = 1 \times 10^{-3} \text{ M}$; (2) $[\text{HSO}_5^-] = 2 \times 10^{-3} \text{ M}$; (3) $[\text{HSO}_5^-] = 3 \times 10^{-3} \text{ M}$; (4) $[\text{HSO}_5^-] = 4 \times 10^{-3} \text{ M}$; (5) $[\text{HSO}_5^-] = 5 \times 10^{-3} \text{ M}$; $\lambda = 390 \text{ nm}$, optical path length 1 cm .

$\text{M}^{-1} \text{ s}^{-1}$. On a longer time scale, the absorbance vs time traces for the subsequent decomposition reaction could be fitted to two exponential functions and both k_{obs} values show a dependence on the HSO_5^- concentration (Figure 3b). The data in Figure 3b suggest that a limiting k_{obs} value is reached at high HSO_5^- concentrations. A nonlinear least-squares fit of the data according to a rate law of the type $k_{\text{obs}} = kK[\text{HSO}_5^-]/(1 + K[\text{HSO}_5^-])$, which is typical for a process consisting of a precursor-formation step followed by a rate-determining elec-

(23) Barefield, E. K.; Lovocchio, F. V.; Tokel, N. E.; Ochiai, E.; Busch, D. H. *Inorg. Chem.* **1972**, *11*, 283.

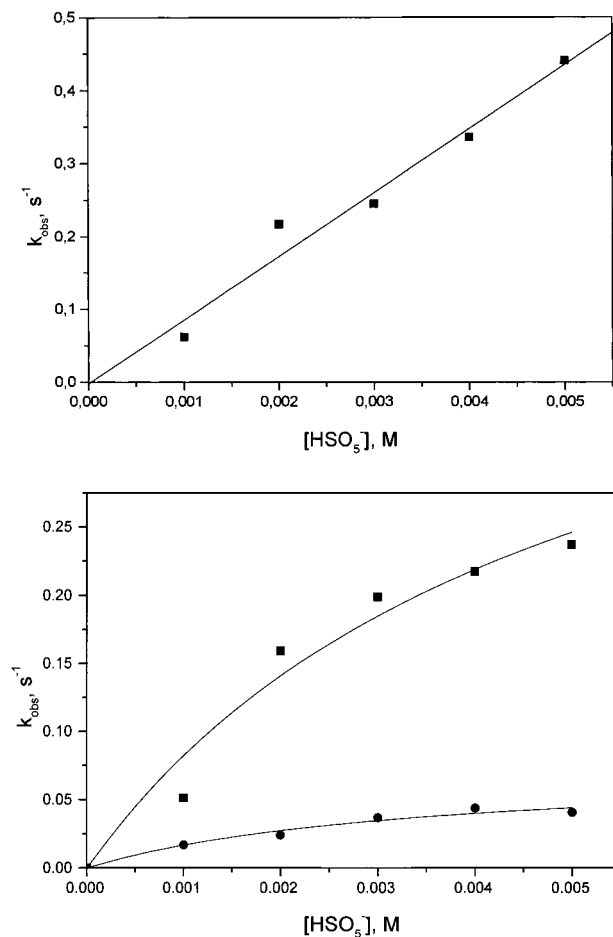


Figure 3. (a) Top: Dependence of k_{obs} for the oxidation of $[\text{NiCR}]^{2+}$ by HSO_5^- on the HSO_5^- concentration. (b) Bottom: Dependence of k_{obs} for the subsequent reactions of $[\text{NiCR}]^{2+}$ with HSO_5^- on the HSO_5^- concentration. Key: ■, fast reaction; ●, slow reaction.

tron transfer reaction, results in $K = 202 \pm 111$ and $295 \pm 130 \text{ M}^{-1}$ and $k = 0.49 \pm 0.16$ and $0.074 \pm 0.016 \text{ s}^{-1}$ for the fast and slow reactions, respectively. It was, however, not possible to fit the complete absorbance vs time traces, as presented in Figure 2c, with three or four exponential functions, presumably due to the similar order of magnitude of some of the rate constants. Nevertheless, the approximate fit of the data does suggest that the formation and decomposition rate constants depend on the HSO_5^- concentration due to the fact that the ligand is capable of undergoing further oxidation.

$[\text{NiKGH-CONH}_2]^+/\text{HSO}_3^-/\text{O}_2$ System. Preliminary experiments demonstrated that the formation of a Ni(III) complex in the reaction between $[\text{NiKGH-CONH}_2]^+$ and sulfite could only be observed in a limited sulfite concentration range in air-saturated solutions. A maximum build up of Ni(III), characterized by a band at 370 nm (see Figure 3 in ref 15), was seen at a S(IV) concentration of 1 mM and a complex concentration of 0.1 mM. At higher sulfite concentrations a similar band was observed, but the overall spectral changes became very broad. Under these conditions the reaction is much faster than for the $[\text{NiCR}]^{2+}$ complex in the presence of air, and the absorbance vs time traces presented in Figure 4a clearly exhibit autocatalytic behavior. There is a decrease in the duration of the induction period with increasing sulfite concentration. The rate constant for the oxidation step following the induction period does not depend significantly on the S(IV) concentration in the range 0.2–2.0 mM and has an average value of $4 \pm 1 \text{ s}^{-1}$ under these conditions. A subsequent slow decomposition with some evidence for redox cycling of the Ni(III) system is observed on

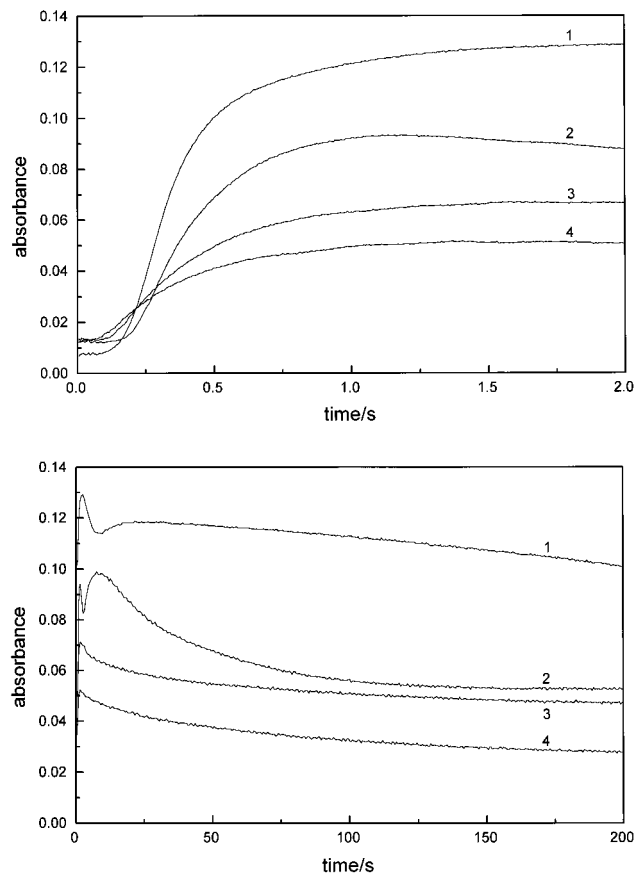


Figure 4. (a) Top: Absorbance–time traces for the oxidation of $[\text{NiKGH-CONH}_2]^+$ by sulfite in the presence of air at different sulfite concentrations. Key: (1) $[\text{S(IV)}] = 0.25 \times 10^{-3} \text{ M}$; (2) $[\text{S(IV)}] = 0.5 \times 10^{-3} \text{ M}$; (3) $[\text{S(IV)}] = 1 \times 10^{-3} \text{ M}$; (4) $[\text{S(IV)}] = 2 \times 10^{-3} \text{ M}$; $\lambda = 370 \text{ nm}$. (b) Bottom: Absorbance–time traces for the subsequent reactions of $[\text{NiKGH-CONH}_2]^+$ with sulfite in the presence of air at different sulfite concentrations. Key: (1) $[\text{S(IV)}] = 0.25 \times 10^{-3} \text{ M}$; (2) $[\text{S(IV)}] = 0.5 \times 10^{-3} \text{ M}$; (3) $[\text{S(IV)}] = 1 \times 10^{-3} \text{ M}$; (4) $[\text{S(IV)}] = 2 \times 10^{-3} \text{ M}$; $\lambda = 370 \text{ nm}$.

a longer time scale (Figure 4b). The influence of the oxygen content of the solution on the observed kinetic trace was also studied. The results indicated that the decomposition reaction was not significantly affected by an increase in oxygen concentration. However, the spectral changes observed for the oxidation of Ni(II) to Ni(III) (formation of a band at 370 nm) became very broad when the oxygen concentration was increased, similar to that observed on increasing the S(IV) concentration.

$[\text{NiKGH-CONH}_2]^+/\text{HSO}_5^-/\text{O}_2$ System. The reaction between $[\text{NiKGH-CONH}_2]^+$ and HSO_5^- results in the very efficient oxidation of Ni(II) to Ni(III). The oxidation is over within 100 ms at 25 °C, and the subsequent decomposition is over within 50 s. Kinetic traces recorded at 15 °C exhibit no induction period and good first-order behavior (Figure 5a). The values of k_{obs} for the formation of Ni(III) show a linear dependence on the HSO_5^- concentration as for the $[\text{NiCR}]^{2+}$ system (Figure 5b) with a slope of $(1.2 \pm 0.1) \times 10^4 \text{ M}^{-1} \text{ s}^{-1}$. Figure 5b clearly exhibits an intercept, which must be due to either a back or parallel reaction. A series of reactions was also studied as a function of the oxygen concentration. Neither the kinetic trace for the oxidation by HSO_5^- nor the calculated first-order rate constant showed any dependence on the oxygen concentration. The subsequent slower decomposition reaction exhibits a characteristic break point that is reminiscent of a similar break point observed in the $\text{Fe(III)/HSO}_3^-/\text{O}_2$ system,

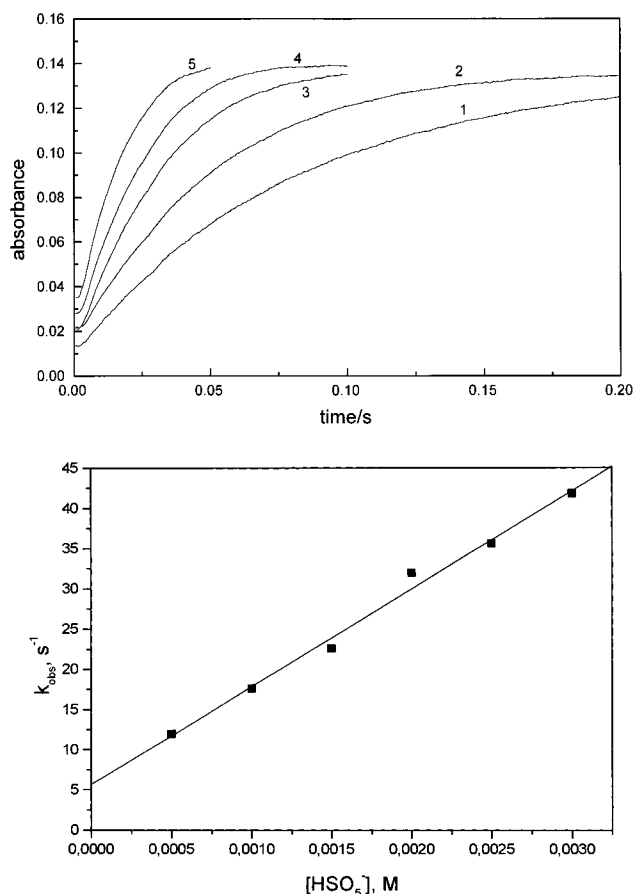


Figure 5. (a) Top: Absorbance–time traces for the oxidation of $[\text{NiKKGH-CONH}_2]^+$ by HSO_5^- in the presence of air at different HSO_5^- concentrations ($[\text{NiKKGH-CONH}_2]^+ = 1 \times 10^{-4} \text{ M}$; $I = 0.2 \text{ M}$; $\text{pH} = 6.5$; $T = 15 \text{ }^\circ\text{C}$). Key: (1) $[\text{HSO}_5^-] = 0.5 \times 10^{-3} \text{ M}$; (2) $[\text{HSO}_5^-] = 1 \times 10^{-3} \text{ M}$; (3) $[\text{HSO}_5^-] = 1.5 \times 10^{-3} \text{ M}$; (4) $[\text{HSO}_5^-] = 2 \times 10^{-3} \text{ M}$; (5) $[\text{HSO}_5^-] = 3 \times 10^{-3} \text{ M}$; $\lambda = 370 \text{ nm}$. (b) Bottom: Dependence of k_{obs} for the oxidation of $[\text{NiKKGH-CONH}_2]^+$ by HSO_5^- on the HSO_5^- concentration.

i.e., a fast decay up to the point where all O_2 in solution has been consumed (see Supporting Information).²⁴

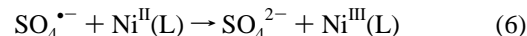
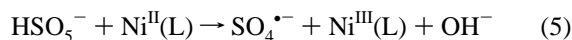
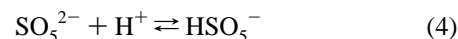
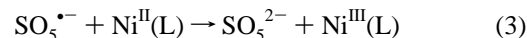
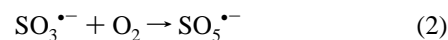
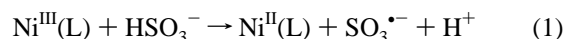
Mechanistic Interpretation. The observed spectral changes on the addition of either $\text{HSO}_3^-/\text{SO}_3^{2-}$ or HSO_5^- in the presence of oxygen to the investigated $\text{Ni}^{\text{II}}(\text{L})$ complexes are interpreted in terms of the formation of $\text{Ni}^{\text{III}}(\text{L})$ complexes, characterized by the formation of a new band around 400 nm, of which the stability will depend on the redox partner and the selected experimental conditions. Similar spectral changes were employed to study the redox cycling of $\text{Ni}^{\text{II/III}}(\text{cyclam})$ in the presence of sulfite and oxygen at low pH.²⁵ In the latter case, it was possible to prepare the Ni^{III} complex separately. In the present study, the $\text{Ni}^{\text{III}}\text{CR}$ complex appears to be formed in a higher steady-state concentration in the presence of sulfite and oxygen (see Figure 1b). That the increase in absorbance in Figure 1b is due to $\text{Ni}^{\text{III}}\text{CR}$ is supported by the fact that Ni^{III} species are known to have higher extinction coefficients at 390 nm, while the oxidized ligand complex, $\text{Ni}^{\text{II}}(\text{CR-2H})$, has essentially a lower extinction coefficient than $\text{Ni}^{\text{III}}\text{CR}$ as seen on the addition of more sulfite to the solution.

The suggested formation of stable or intermediate Ni^{III} complexes must depend on the driving force of the redox partners. The driving force of $\text{SO}_5^{\bullet-}$ (1.1 V vs NHE)²⁶ is too

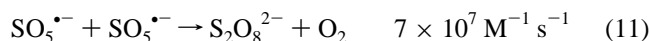
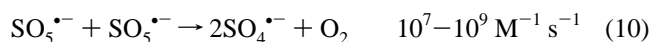
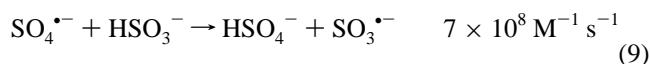
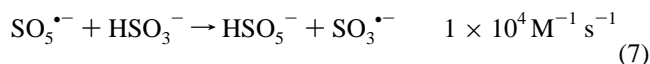
low to oxidize $[\text{NiCR}]^{2+}$ (ca. 1.3 V),¹⁵ whereas the driving forces of HSO_5^- (1.8 V)²⁶ and $\text{SO}_4^{\bullet-}$ (2.5 V)²⁶ are high enough to oxidize this complex. In the case of the $[\text{NiKKGH-CONH}_2]^+$ complex, a much lower driving force is required (ca. 0.9 V),¹⁵ and all three mentioned species are in principle suitable. Earlier studies on DNA damage in the presence of the investigated systems^{14,15} revealed evidence for the participation of $\text{SO}_4^{\bullet-}$ radicals only in the $[\text{NiCR}]^{2+}/\text{HSO}_3^-/\text{SO}_3^{2-}/\text{O}_2$ system. This is also the only case where a stable Ni^{III} species could be observed.

We now turn to plausible reaction mechanisms based on available literature data that can account for the observed kinetic observations in a qualitative way.

$\text{Ni}^{\text{III}}(\text{L})/\text{HSO}_3^-/\text{SO}_3^{2-}/\text{O}_2$ Systems. For both complexes a clear induction period is observed and the corresponding rate constant for the formation of $\text{Ni}^{\text{III}}(\text{L})$ does not depend on the sulfite concentration. The traces for $[\text{NiCR}]^{2+}$ indicate an initial decrease in absorbance, which suggests that there could be some Ni^{III} in solution. This is understandable since the $[\text{Ni}^{\text{III}}\text{CR}]^{3+}$ complex is somewhat more stable and does not undergo rapid decomposition, in contrast to the situation when excess HSO_5^- is present in the medium. The mechanism must include the following steps:



In the case of the $[\text{NiCR}]^{2+}$ complex, only reactions 5 and 6 can in principle account for the oxidation of Ni^{II} to Ni^{III} . Since reaction 2 is very rapid ($1.5 \times 10^9 \text{ M}^{-1} \text{ s}^{-1}$),²⁷ reaction 3 will control the formation of HSO_5^- and $\text{SO}_4^{\bullet-}$. Therefore, these species must be formed in reactions involving sulfite and $\text{SO}_5^{\bullet-}$ as shown in (7), (8), and (10), respectively. The quoted



rate constants at 25 °C are taken from literature in which these experimental values seemed to fit in well with model calculations.^{24,28} The subsequent decomposition of Ni^{III} must involve reaction 1 in the presence of an excess of $\text{HSO}_3^-/\text{SO}_3^{2-}$. The $[\text{Ni}^{\text{III}}\text{CR}]^{3+}$ complex can obviously not be reduced by $\text{S}(\text{IV})$ in competition with its reoxidation (from Ni^{II}) by HSO_5^- and $\text{SO}_4^{\bullet-}$ on the basis of the quoted redox potentials. Thus, depending on the selected experimental conditions, which will control the

(24) Brandt, C.; Fabian, I.; van Eldik, R. *Inorg. Chem.* **1994**, *33*, 687.

(25) Linn, D. E.; Dragan, M. J.; Miller, D. E. *Inorg. Chem.* **1990**, *29*, 4356.

(26) Reference 3, Table 3.5.

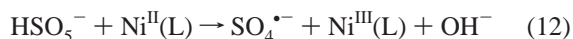
(27) Neta, P.; Huie, R. E.; Ross, A. B. *J. Phys. Chem. Ref. Data* **1988**, *17*, 1027.

(28) Warneck, P.; Ziajka, J. *Ber. Bunsen-Ges. Phys. Chem.* **1995**, *99*, 59.

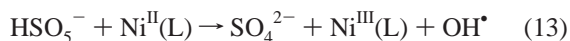
competition between formation and decomposition of $[\text{Ni}^{\text{III}}\text{CR}]^{3+}$, a situation can be reached where $[\text{Ni}^{\text{III}}\text{CR}]^{3+}$ is relatively stable over a longer period of time (see Figure 1b). The induction period observed for both complexes must involve the formation of the species capable of oxidizing $\text{Ni}^{\text{II}}(\text{L})$ to $\text{Ni}^{\text{III}}(\text{L})$, i.e., $\text{SO}_5^{\bullet-}$, HSO_5^- , and $\text{SO}_4^{\bullet-}$ for $[\text{NiKGH-CONH}_2]^+$ and HSO_5^- and $\text{SO}_4^{\bullet-}$ for $[\text{NiCR}]^{2+}$, respectively.

In the case of the $[\text{NiKGH-CONH}_2]^+$ complex, the $[\text{HSO}_3^-/\text{SO}_3^{2-}]:[\text{O}_2]$ ratio also plays an important role. This must be related to the interference of the subsequent reactions (7), (8), (10), and (11) in which $\text{SO}_5^{\bullet-}$ is used up and will then not be available for the effective oxidation of $[\text{Ni}^{\text{II}}\text{KGH-CONH}_2]^+$ to $[\text{Ni}^{\text{III}}\text{KGH-CONH}_2]^{2+}$. The oxidation of $[\text{Ni}^{\text{II}}\text{KGH-CONH}_2]^+$ is at least 10^2 times faster than the oxidation of $[\text{Ni}^{\text{II}}\text{CR}]^{2+}$, where the latter requires a high oxygen concentration, i.e. an effective formation of $\text{SO}_5^{\bullet-}$ in reaction 2. This is directly related to the required redox potential as outlined above.

$\text{Ni}^{\text{II}}(\text{L})/\text{HSO}_5^-$ Systems. Both complexes show no induction period during reaction with peroxymonosulfate, and the buildup of $\text{Ni}^{\text{III}}(\text{L})$ is followed by a subsequent decomposition back to $\text{Ni}^{\text{II}}(\text{L})$. The oxidation process depends linearly on the HSO_5^- concentration, and the second-order rate constant is ca. $10^2 \text{ M}^{-1} \text{ s}^{-1}$ for the $[\text{NiCR}]^{2+}$ complex and ca. $2 \times 10^4 \text{ M}^{-1} \text{ s}^{-1}$ for the $[\text{NiKGH-CONH}_2]^+$ complex at 25 °C. In the case of the $[\text{NiKGH-CONH}_2]^+$ complex evidence for the existence of a back or parallel reaction was observed in the form of an intercept in Figure 5b. The parallel reaction could involve a rate-determining intramolecular rearrangement of the complex or a solvolysis process prior to the oxidation step. The subsequent decomposition reactions occur on the same time scale (ca. 40–50 s), and a characteristic break point is observed in the case of the $[\text{NiKGH-CONH}_2]^+$ complex, which could indicate the occurrence of a redox cycle of the nickel complex during the decomposition reaction. The formation of $\text{Ni}^{\text{III}}(\text{L})$ must involve the following reaction:



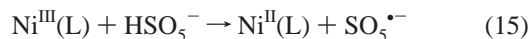
or



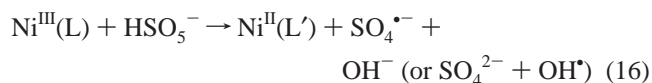
In this reaction the $\text{SO}_4^{\bullet-}$ radical presumably remains coordinated to the $\text{Ni}^{\text{III}}(\text{L})$ complex since no evidence for the presence of the free radical was found.¹⁵ Reaction 13 leading to hydroxyl radicals can be ruled out in this case since no evidence for its formation could be detected in DNA experiments.¹⁵



The decomposition of the $\text{Ni}^{\text{III}}(\text{L})$ or $\text{Ni}^{\text{IV}}(\text{L})$ species must involve reduction by for instance HSO_5^-



or



where L' represents the oxidized form CR-2H of the ligand in the case of the NiCR system. $\text{SO}_5^{\bullet-}$ and $\text{SO}_4^{\bullet-}$ are strong oxidants and can initiate redox cycling of $\text{Ni}^{\text{II}}(\text{L})$ to $\text{Ni}^{\text{III}}(\text{L})$. The details of this decomposition reaction are presently unknown, and it may also involve reduction by $\text{SO}_4^{\bullet-}$ or HSO_3^- , etc. In addition, it may also involve the oxidation of the ligand,

which will lead to decomposition of the $\text{Ni}^{\text{III}}(\text{L})$ species. Similar reactions were suggested to account for the redox cycling of $\text{Ni}^{\text{II}}(\text{cyclam})$ during the catalyzed autoxidation of sulfite,²⁵ although no evidence for the decomposition of the chelate ligand was reported.

Reactions 15 and 16 can in principle account for the nonlinear dependence of k_{obs} on the HSO_5^- concentration reported in Figure 3b. The calculated values for the precursor formation constant (K) are quite large and indicate an effective interaction between the redox partners, followed by a rate-determining electron-transfer process. At present it is not possible to assign these reactions to a specific one of the fast or slow kinetic steps observed.

Evidence for the formation of $\text{SO}_4^{\bullet-}$ radicals was obtained in the $[\text{NiCR}]^{2+}/\text{HSO}_3^-/\text{SO}_3^{2-}/\text{O}_2$ system, but not in the other three systems.¹⁵ The $[\text{NiCR}]^{2+}/\text{HSO}_3^-/\text{SO}_3^{2-}/\text{O}_2$ system is the only one that forms a relatively stable $\text{Ni}^{\text{III}}(\text{L})$ species. The other three systems all show relatively fast subsequent decomposition reactions, and here the participation of $\text{SO}_4^{\bullet-}$ could not be proven. Thus, there may be a link between the stability of the $\text{Ni}^{\text{III}}(\text{L})$ species and the ability to detect $\text{SO}_4^{\bullet-}$ radicals in solution.

The redox cycling observed for a number of systems in the present study may, in part, account for the efficient oxidation of guanine in DNA.¹⁵ The kinetic studies described here confirm that both $[\text{NiCR}]^{2+}$ and $[\text{NiKGH-CONH}_2]^+$ react quickly and without an induction period with peroxymonosulfate, HSO_5^- , generating a $\text{Ni}(\text{III})$ species that undergoes subsequent decomposition involving either ligand degradation or, in the presence of DNA, guanine oxidation. In contrast, the two nickel complexes behave somewhat differently in their reactions with $\text{S}(\text{IV})$ and O_2 . Both systems display an induction period which must be related to the generation of sufficient concentrations of $\text{Ni}(\text{III})$ to promote one-electron oxidation of $\text{HSO}_3^-/\text{SO}_3^{2-}$ leading to a rapid reaction with O_2 . On the other hand, the complexes differ in their subsequent chemistry with the $\text{SO}_5^{\bullet-}$ so formed. In the case of the nickel peptide complex, $\text{SO}_5^{\bullet-}$ is reduced by $\text{Ni}^{\text{II}}\text{L}$ to regenerate the catalytic $\text{Ni}^{\text{III}}\text{L}$, forming the strong oxidant HSO_5^- , which is known to oxidize guanine residues in DNA in the presence of nickel complexes. The reduction of $\text{SO}_5^{\bullet-}$ is sensitive to the relative concentrations of $\text{S}(\text{IV})$ and O_2 because of the various competing pathways for $\text{SO}_5^{\bullet-}$ decomposition (eqs 7, 8, 10, 11) in the presence of excess sulfite, and this dependence on $[\text{S}(\text{IV})]:[\text{O}_2]$ is also seen in DNA reactions.¹⁵ In contrast, $[\text{Ni}^{\text{II}}\text{CR}]^{2+}$ cannot easily reduce $\text{SO}_5^{\bullet-}$ because of its higher $\text{Ni}^{\text{III/II}}$ redox potential compared to $[\text{Ni}^{\text{II}}\text{KGH-CONH}_2]^+$, so that sulfate radicals formed from eqs 8 and 10 are observed instead. In the presence of DNA, $\text{SO}_4^{\bullet-}$ leads to guanine oxidation; in the absence of DNA as studied here, $\text{SO}_4^{\bullet-}$ may reoxidize $[\text{Ni}^{\text{II}}\text{CR}]^{2+}$. In summary, both nickel complexes undergo redox cycling during the course of sulfite autoxidation; however, somewhat different reactive intermediates, namely the presence or absence of substantial concentrations of $\text{SO}_4^{\bullet-}$, appear to be involved for $[\text{NiCR}]^{2+}$ and $[\text{NiKGH-CONH}_2]^+$, respectively.

Acknowledgment. Support of this work by grants from the Deutsche Forschungsgemeinschaft, DAAD, Volkswagen Foundation (to R.v.E.) and the National Institutes of Health (GM-49860 to C.J.B.) is gratefully acknowledged. We thank Ms. Danielle Bodrero-Hoggan for preparation of KGH-CONH_2 .

Supporting Information Available: An absorbance–time trace for reaction of $[\text{NiKGH-CONH}_2]^+$ with HSO_5^- in air. This material is available free of charge via the Internet at <http://pubs.acs.org>.